Bioelectrochemistry 74 (2008) 111–117

Contents lists available at ScienceDirect

Bioelectrochemistry

journal homepage: www.elsevier.com/locate/bioelechem

DNA-programmable multiplexing for scalable, renewable redox protein bio-nanoelectronics

Gary D. Withey [a,*], Jin Ho Kim [b], Jimmy Xu [b]

[a] Biomedical Engineering Program, Brown University, 184 Hope Street, Providence, Rhode Island 02912, USA
[b] Division of Engineering and Department of Physics, Brown University, 184 Hope Street, Providence, Rhode Island 02912, USA

ARTICLE INFO

Article history:
Received 27 November 2007
Received in revised form 21 February 2008
Accepted 9 May 2008
Available online 21 May 2008

Keywords:
Biosensor
Carbon nanotube
Enzyme
Direct electron transfer
Self-assembly

ABSTRACT

A universal, site-addressable DNA linking strategy is deployed for the programmable assembly of multifunctional, long-lasting redox protein nanoelectronic devices. This addressable linker, the first incorporated into a redox enzyme-nanoelectronic system, promotes versatility and renewability by allowing the reconfiguration and replacement of enzymes at will. The linker is transferable to all redox proteins due to the simple conjugation chemistry involved. The efficacy of this linking strategy is assessed using two model enzymes, glucose oxidase (GOx) and alcohol dehydrogenase (ADH), self-assembled onto separate nanoelectrode regions comprised of a highly ordered carbon nanotube (CNT) array. The sequence-specificity of DNA hybridization provides the means of encoding spatial address to the self-assembling process that conjugates enzymes tagged with single-stranded DNA (ssDNA) to the tips of designated CNTs functionalized with the complementary strands. In this study, we demonstrate the feasibility of multiplexed, scalable, reconfigurable and renewable transduction of redox protein signals by virtue of DNA addressing.

© 2008 Elsevier B.V. All rights reserved.

1. Introduction

Though the subject of bioelectronics has been pursued for decades, interest in the field has redoubled since the arrival of nanomaterials such as CNTs that have been shown not only to be a superb passive electrical conduit but also to promote electron transfer from enzymes [1–6]. For all that the technology has advanced in recent years, the resulting devices have often been discrete and singular in function and are only useful over a very short lifespan [7,8]. Methods that would enable integration and scalability to multifunctional devices have been the missing link that is critical for the evolution of more sophisticated nanoelectronic circuit platforms. Moreover, the dependence of bioelectronic devices on biomolecules as fragile as redox enzymes demands that an additional challenge be addressed – facilitated protein detachment and replacement – to extend the lifetime of these devices. Enzymes immobilized on an electrode retain their activity typically for periods on the order of only days to weeks [7,8]. After that time the device loses its activity and would have to be discarded unless the denatured protein can be replaced with fresh enzymes. To remove protein that is covalently bound to a CNT electrode typically requires an aggressive acid washing procedure that not only leaves protein residue and dislodged redox cofactors that can cloud future measurements, but also degrades the underlying electrode surface itself [9]. An alternate, more reversible means of protein immobilization must be developed in order to make these devices truly reusable. There have been many studies involving synthetic DNA oligos used as molecular linkers to tether together different molecules, nanoparticles and nanotubes [10–12]. In these linking schemes, the components are tagged with complementary DNA single strands, and hybridization of the strands joins the components. The reversibility of DNA hybridization allows this link to be broken without the harsh treatment necessary to break a covalent bond; a functionalized nanoelectrode array chip that incorporates DNA as a molecular link between the enzyme and the electrode surface could be cleaned with a simple deionized water (DIH_2O) washing procedure or NaOH dehybridization wash [11]. The most important role for the DNA link is enabling the simultaneous, parallel, site-addressable binding of multiple different redox proteins to designated nanoelectrode regions. In this linking scheme, oligos of differing sequences provide distinct DNA 'addresses' to different regions of a highly ordered template-grown CNT array nanoelectrode. Details of the fabrication of this CNT array have been published previously [13]. Enzymes labeled with the complementary ssDNA tags will recognize their binding address and assemble to that specific region. The result is a single bio-nanoelectronic array multi-functionalized with several different redox enzymes that are capable of real-time screening for multiple substances in parallel (Fig. 1a). Two enzymes, GOx and ADH, were selected as model proteins in this study to demonstrate the site-addressability and scalability enabled by this approach. The resulting bio-nanoelectronic prototype device is a

* Corresponding author. Tel.: +1 4018633010; fax: +1 4018639107.
E-mail address: gary_withey@brown.edu (G.D. Withey).

1567-5394/$ – see front matter © 2008 Elsevier B.V. All rights reserved.
doi:10.1016/j.bioelechem.2008.05.004

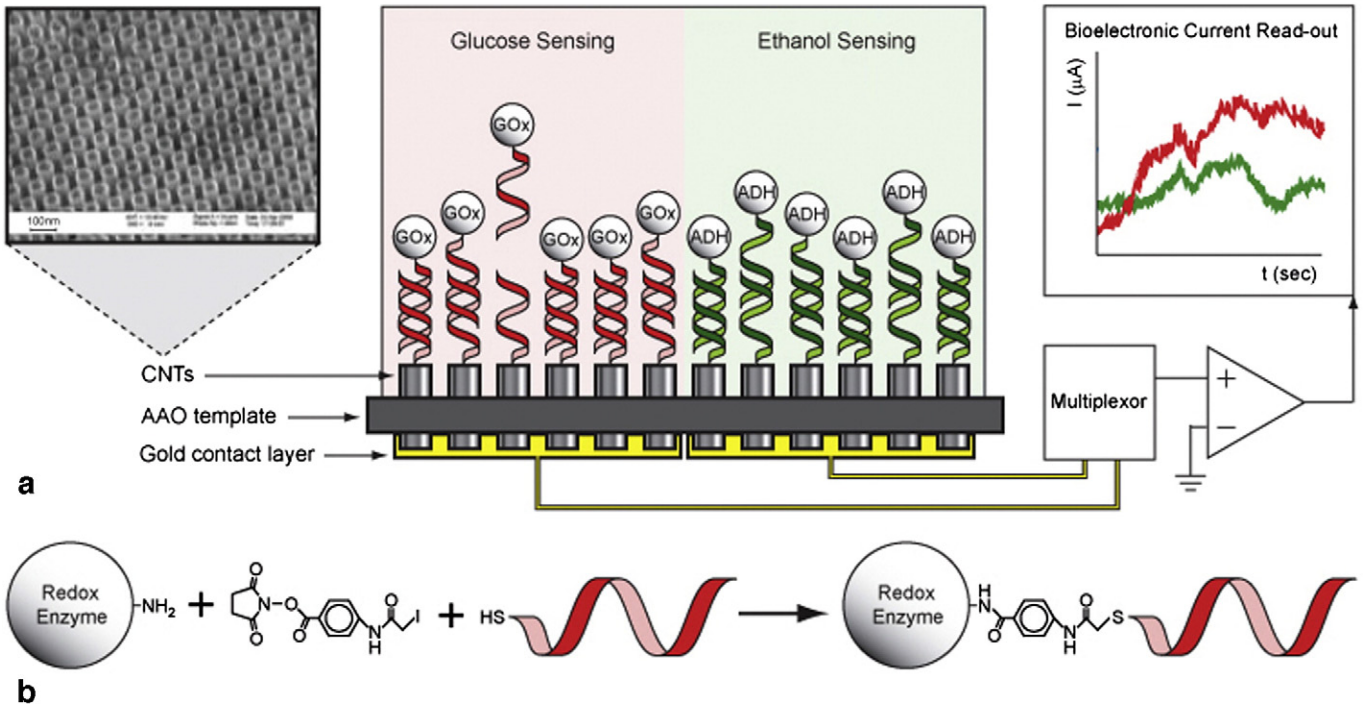

Fig. 1. (a) A multiplexed redox enzyme biosensor enabled by DNA-directed assembly (center). Individually electrically contacted sensing regions each produce a bioelectrocatalytic current (right) that is indicative of the concentration of its respective substrate (e.g. glucose, ethanol). Left, a scanning electron micrograph of the highly ordered CNT array used in this study (scale bar = 100 nm). (b) SIAB as an enzyme–DNA crosslinker.

multiplexed biosensor for the real-time detection of glucose and ethanol.

Redox protein biosensors electrochemically monitor the rate of turnover of a redox reaction at an enzyme-linked electrode surface in the presence of its substrate [7,8]. In the case of GOx, the $FADH_2$ redox center is oxidized at +0.24 V, transferring two electrons to the electrode under anaerobic conditions [14]. FAD is then reduced back to $FADH_2$ by the oxidation of glucose to gluconate. The reaction will continually turn over in the presence of glucose, and the rate of turnover is directly related to the glucose concentration up to the point of saturation. The anodic current measured through the electrode is therefore a direct measure of the glucose concentration. For the GOx–CNT system, this overpotential (+0.24 V from the −0.6 V redox potential of free FAD) arises from the electron transfer barrier at the GOx–CNT interface. Redox potentials as high as +0.65 V have been reported for such systems [2,15,16]. Conversely, immobilization on CNT nanoelectrodes has been demonstrated to promote substantial negative shifts in the anodic peak potentials of dehydrogenases such as ADH [17,18], and we have found that to be the case in this study with an observed redox potential of 0.18 V vs. Ag/AgCl.

2. Materials and methods

2.1. Electrode construction

The electrodes used in this study were constructed using CNT array samples as the working electrode surface. The CNT array is fabricated by a two-step anodization of high purity aluminum foil (~99.999%, ESPI) followed by CNT growth by a chemical vapor deposition (CVD) process. The aluminum foil is first anodized in a 0.3 M oxalic acid solution (Sigma) at 10 °C under a constant voltage of 40 V for 16 h using an in-house built electrochemical cell consisting of a water-jacketed beaker and graphite sheet electrodes, and a Sorensen power supply (DCS80-13). This anodized layer of aluminum oxide is then removed in a solution of 6% H_3PO_4 and 1.8% CrO_3 (Sigma) at 60 °C. A second anodization is carried out in a 0.3 M oxalic acid solution at 10 °C under a constant voltage of 40 V for 5 h, resulting in a highly ordered, hexagonal array of parallel, vertically-oriented pores. A small amount of cobalt catalyst (Sigma) is then electrochemically deposited into the bottom of the template channels using a 100 Hz, 14 V AC power supply (HP, 3310A and Kepco, BOP 100-4M) in a solution of 4% H_3PO_4, 12% $CoSO_4$ and 0.1% ascorbic acid (Sigma). The remaining Al metal layer is removed by 1% $HgCl_2$ (Sigma). To grow CNTs from the nanopores, the deposited catalyst is reduced by heating in a tube CVD furnace (Tec-Vac Industries) at 630 °C for 4 h under a CO flow of 100 $cm^3 \cdot min^{-1}$. The CO flow is then replaced by a mixture of 10% acetylene in nitrogen gas at a flow rate of 100 $cm^3 \cdot min^{-1}$ and is maintained for 2 h at 650 °C. After CNT growth, the amorphous glassy carbon layer on the surface is removed by reactive ion etching (Trion Technology) using BCl_3 (Sigma). CNTs were exposed from the template pores by a length of 50 nm using a 6% H_3PO_4, 1.8% CrO_3 chemical etch for 10 h at 25 °C to remove a layer of the anodized aluminum oxide (AAO) template. Further detail of the CNT array fabrication and post-fabrication processing has been published previously by our group [13]. To provide an electrical contact to the CNTs, a 100 nm gold layer was deposited onto the backside of the array using an e-beam evaporator (Thermionics Laboratory). A gold wire (0.127 mm, ESPI) was attached to this gold layer with silver paint (SPI Supplies), and the wire was threaded through a glass tube (1.5 mm, Sutter Instrument). The contact interface between the array and the glass tube was sealed with hot glue (McMaster-Carr) to prevent exposure of the bare gold layer, gold wire or silver paint to the electrochemistry solutions.

2.2. Enzyme–DNA crosslinking

All oligonucleotides used in this study were synthesized by Proligo (Sigma). The thiolated oligos seqA' and seqB' were adapted from sequences proven to exhibit high hybridization efficiency [19]. GOx from *Aspergillus niger* (Sigma) and ADH from *Saccharomyces cerevisiae*

(Sigma) were dissolved in separate solutions of 50 mM, pH 8.3 sodium borate buffer (Sigma) and 5 mM EDTA (Sigma) to final protein concentrations of 0.1 mg/ml each. SIAB (Pierce) was dissolved in DMSO (Sigma) to make a 3.5 mM stock solution. 3 μl of SIAB stock was added to 1 ml of each protein solution, and the mixtures were allowed to react for 30 min at 25 °C. Two 1 ml Micro DispoDialyzers (Spectrum Laboratories) with a molecular weight cut-off (MWCO) of 3.5 kDa were conditioned using 50 mM sodium borate buffer, pH 8.3 for 30 min. The reaction mixtures were then transferred to the DispoDialyzer tubing to remove excess SIAB by dialysis at 4 °C for 12 h against a borate buffer solution, changing the 500 ml dialysis bath three times. The thiolated oligos seqA' and seqB' were then added to the GOx and ADH reaction mixtures, respectively, to a final concentration of 1 μM and allowed to react for 1 h at 25 °C in the dark. To cap any unreacted iodoacetyl groups on the SIAB crosslinker, cysteine (Pierce) was then added to the reaction mixtures to a final concentration of 5 mM and reacted for 15 min at 25 °C in the dark. Two 1 ml, 25 kDa MWCO Micro DispoDialyzer were conditioned to a 10 mM sodium phosphate buffer, 150 mM NaCl, pH 7.4 solution (PBS) (Sigma) for 30 min. Unreacted oligos and excess cysteine were removed by dialysis of the reaction mixtures in the DispoDialyzer and a 500 ml PBS dialysis bath at 4 °C, changed three times over 12 h. Enzyme–DNA conjugates were stored at 4 °C in PBS.

2.3. DNA addressing and hybridization

CNTs were functionalized with carboxylic acid groups by etching for 2 h in a 6 M H_2SO_4, 2 M HNO_3 solution (Sigma). The amine-terminated oligos seqA and seqB were covalently bound to the CNT array electrode to direct the assembly of their complements, seqA' and seqB', to their respective sites. The covalent attachment was performed by first incubating the COOH-functionalized CNT array in 1-ethyl-3-(3-dimethylaminopropyl) carbodiimide hydrochloride (EDC, 200 mM, Biacore), *N*-hydroxysuccinimide (NHS, 50 mM, Biacore) and 2-(*N*-morpholino)ethanesulphonic acid (MES, 50 mM, Sigma) buffer for 1 h at 25 °C to form reactive esters from the carboxylic acid groups. The amine-terminated oligo was then added and incubated for 2 h at 25 °C to allow covalent binding. To prevent adsorption to the CNT side-walls, the CNT array was treated with GA (0.1% in PBS, pH 7.0, Aldrich), and subsequently washed with PBS to remove excess surfactant. Hybridization of enzyme–DNA conjugates to the DNA-functionalized CNT array occurred in 100 mM NaCl, 50 mM phosphate buffer at pH 7.0, at an enzyme–DNA conjugate concentration of 0.1 mg/ml. The solution was heated to 40 °C and allowed to cool slowly to room temperature. Following hybridization, the CNT array was washed with hybridization buffer to remove unbound enzyme–DNA conjugates. Inactive conjugate was dehybridized and removed by washing the electrode in a 1 l DIH_2O bath at 65 °C, stirring constantly for 1 h. For parallel addressing of multiple nanoelectrode regions, seqA and seqB were physically spotted onto separate, individually electrically contacted regions of CNT array. The electrode was then immersed in a hybridization bath containing both GOx–seqA' and ADH–seqB'. Hybridization conditions were applied as previously described (vide supra). Enzymes were assembled to their respective binding sites by sequence-specific hybridization.

2.4. Electrochemical measurements

All electrochemical measurements were recorded using a BAS potentiostat C3 cell stand with a three electrode system consisting of the CNT array electrode as the working electrode, a platinum wire auxiliary electrode and a Ag/AgCl reference electrode. Unless otherwise stated, all potentials are reported vs. Ag/AgCl. All trials were run in a 100 mM NaCl, 50 mM phosphate buffer at pH 7.0 (Sigma) and 25 °C. The solution was deoxygenated by bubbling the solution with argon for 20 min. For glucose detection, β-D(+)glucose (Sigma) was used as a substrate. In galactose control experiments, D-(+)-galactose was purchased from Sigma. Ethanol detection was performed in the presence of 100 mM β-nicotinamide adenine dinucleotide (NAD, Sigma), which acts as a cofactor in the oxidation of ethanol to acetaldehyde. CV measurements were taken between −0.8 V and 0.8 V at a scan rate of 50 $mV{\cdot}s^{-1}$. During chronoamperometric measurements, redox potentials of 0.24 V and 0.18 V were applied to the CNT electrode surfaces modified with GOx and ADH, respectively, and the solution was stirred constantly using a magnetic stirrer.

2.5. Calculation of surface coverage of active GOx

To determine the amount of active GOx that is successfully electrically contacted to the electrode surface we take CV measurements, first of the bare CNT electrode (we call this "curve A") and then of the electrode after hybridizing GOx to the CNTs ("curve B"). This measurement is taken in the absence of glucose so that the reaction does not turn over. This way, exactly two electrons are donated by each $FADH_2$ redox center that is successfully electrically contacted to the CNTs. Using curve A as a baseline, the anodic current peak observed on curve B is representative of the total electrocatalytic current drawn from GOx. By dividing the *x*-axis (currently in units of V) by the scan rate used during the CV measurements (in units of $V{\cdot}s^{-1}$), we convert the *x*-axis into units of time (s). The next step is to calculate the area of the peak by integration. This area will carry units of A s. This is equivalent to coulombs, since:

$$A{\cdot}s = (C{\cdot}\,s^{-1}){\cdot}s = C$$

We know that:

$$1C = 6.25 \times 10^{18} e^-$$

$$1e^- = 1.6 \times 10^{-19} C$$

This allows us to calculate the total number of electrons transferred. Since each FAD center donates two electrons and there are two FAD units per dimer of GOx, we can calculate the total number of active GOx present. Dividing this value by the total active electrode surface area gives us the average surface coverage of active GOx. The calculation has been detailed below:

Integration of anodic current peak:

$$3.58 \times 10^{-9}\,A{\cdot}s = 3.58 \times 10^{-9}\,e^-$$

$$\left(3.58 \times 10^{-9}\,C\right) \times \left(6.25 \times 10^{18}\,e^-/C\right) = 2.2 \times 10^{10}\,e^-$$

$$\left(2.2 \times 10^{10}\,e^-\right)/(2\,e^-/FAD) = 1.1 \times 10^{10}\,GOx$$

$$\left(1.1 \times 10^{10}\,GOx\right)/\left(6.02 \times 10^{23}\,GOx/mol\right) = 1.8 \times 10^{-14}\,mol$$

$$\left(1.8 \times 10^{-14}\,mol\right)/(0.0143\,cm^2) = 1.3 \times 10^{-12}\,mol{\cdot}\,cm^{-2}$$

ADH can be quantified by the same method, using a form of the enzyme with the NAD cofactor bound in the active site. This method

Table 1
DNA oligonucleotide sequences

Name	Sequence	Modification
seqA	5′-GGTCCATTTCACACAGGA-3′	5′-amine
seqA'	5′-TCCTGTGTGAAATGGACC-3′	5′-thiol
seqB	5′-GTCAGCTGTGACCGTGAC-3′	5′-amine
seqB'	5′-GTCACGGTCACAGCTGAC-3′	5′-thiol

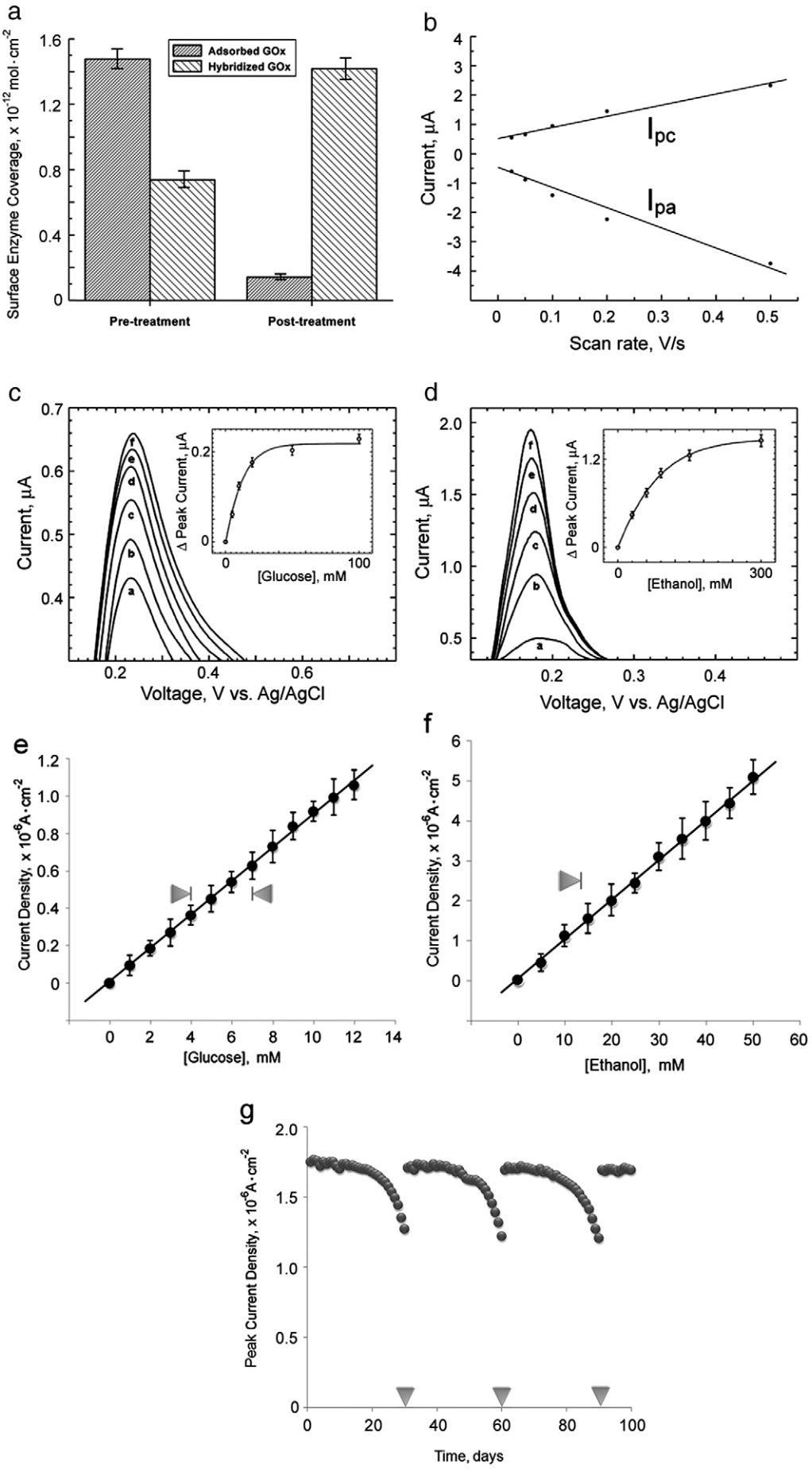
a
Surface Enzyme Coverage, x 10^-12 mol·cm^-2
Adsorbed GOx
Hybridized GOx
Pre-treatment
Post-treatment
b
Current, µA
Ipc
Ipa
Scan rate, V/s
c
Current, µA
Δ Peak Current, µA
[Glucose], mM
Voltage, V vs. Ag/AgCl
d
Current, µA
Δ Peak Current, µA
[Ethanol], mM
Voltage, V vs. Ag/AgCl
e
Current Density, x 10^-6 A·cm^-2
[Glucose], mM
f
Current Density, x 10^-6 A·cm^-2
[Ethanol], mM
g
Peak Current Density, x 10^-6 A·cm^-2
Time, days

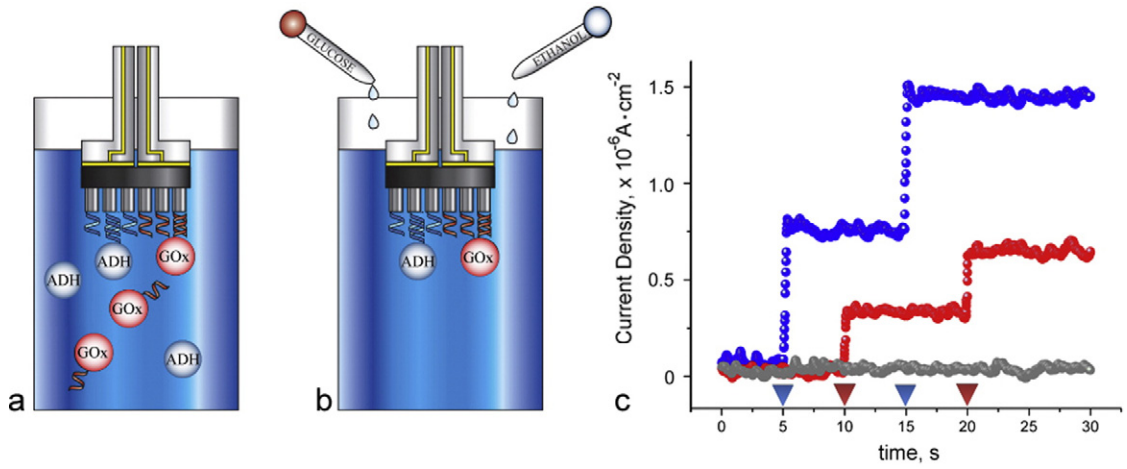

Fig. 3. (a) GOx and ADH assemble to the surfaces modified with the complements to their oligo tags to create a glucose and ethanol biosensor, respectively. (b) Unbound enzyme is washed away and chronoamperometric (CA) measurements are taken on the two sensor surfaces as glucose and ethanol are injected into the common electrochemical solution at discrete time intervals. (c) Results of CA measurements on the GOx sensor (red) at 0.24 V vs. Ag/AgCl and on the ADH sensor (blue) at 0.18 V vs. Ag/AgCl, and a seqA-modified electrode with no bound enzyme (gray) at 0.24 V vs. Ag/AgCl in 100 mM NAD, while glucose and ethanol solutions are injected (For interpretation of the references to color in this figure legend, the reader is referred to the web version of this article.)

for surface enzyme concentration has been demonstrated numerous times in literature [20,21].

2.6. Calculation of k_{ET}

The electron transfer rate can be determined by dividing the peak anodic current density by the active surface enzyme coverage, followed by a few simple conversions. This calculation has been detailed below using GOx as an example:

Peak anodic current	2.46×10^{-8} A
Active electrode surface area	0.0143 cm^2
Anodic current density	$\left(2.46\times10^{-8}\text{ A}\right)/\left(0.0143\text{ cm}^2\right)$
	$=1.72\times10^{-6}\text{ A}\cdot\text{ cm}^{-2}$

Then:

$$1.72\times10^{-6}\text{ A}\cdot\text{ cm}^{-2}=1.72\times10^{-6}\text{ C}\cdot\text{ s}^{-1}\cdot\text{ cm}^{-2}$$
$$\left(1.72\times10^{-6}\text{ C}\cdot\text{ s}^{-1}\cdot\text{ cm}^{-2}\right)/\left(1.6\times10^{-19}\text{ C}\cdot\text{ e}^{-1}\right)=1.08\times10^{13}\text{ e}^{-1}\cdot\text{ s}^{-1}\cdot\text{ cm}^{-2}$$
$$\left(1.3\times10^{-2}\text{ mol}\cdot\text{ cm}^{-2}\right)\times\left(6.02\times10^{23}\text{ GOx/mol}\right)=7.83\times10^{11}\text{ GOx}\cdot\text{ cm}^{-2}$$
$$\left(1.08\times10^{13}\text{ e}^{-1}\cdot\text{ s}^{-1}\cdot\text{ cm}^{-2}\right)/\left(7.83\times10^{11}\text{ GOx}\cdot\text{ cm}^{-2}\right)=13.8\text{ e}^{-}\cdot\text{ s}^{-1}\cdot\text{ GOx}^{-1}$$
$$\rightarrow k_{ET}=13.8\text{ s}^{-1}$$

The electron transfer rate for ADH can be determined by the same method, which has been used repeatedly in literature for k_{ET} calculation [22].

3. Results and discussion

3.1. Reducing protein adsorption through surfactant use

To incorporate the DNA link in our multiplexed biosensor design, two sets of complementary oligo pairs were used (Table 1). Amine-terminated sequence A (seqA) and sequence B (seqB) are covalently linked to the tips of a vertically standing array of CNTs by a carboxyl–amine coupling reaction [2,23] to provide distinguishable DNA addresses to designated binding sites. The corresponding thiolated complements sequence A' (seqA') and sequence B' (seqB') are used to tag the redox enzymes GOx and ADH, respectively. Fig. 1a indicates that the multiple sensing regions are tagged with distinct DNA addresses (color-coded) and oligo-tagged redox enzymes are delivered to their respective target regions by sequence-specific assembly to the sensor surface. We used the heterobifunctinal crosslinking agent *N*-Succinimidyl[4-iodoacetyl]aminobenzoate (SIAB) to attach DNA tags to redox enzymes. This linker ensures the covalent binding of an amino group of the protein at its *N*-succinimidyl ester and the thiolated terminus of a DNA oligo at its iodoacetyl end (Fig. 1b) [24]. Since all proteins contain amine groups on their N-terminus and lysine, arginine, glutamine and asparagine residues [25], SIAB can act as a universal crosslinker for all redox proteins and thiolated DNA oligos. It should be noted that crosslinking reactions can potentially compromise the specificity of redox enzymes. However, control experiments on the GOx system using D-(+)-galactose as a substrate have shown no significant substrate concentration-dependent amperometric response (data not shown), indicating that the enzyme maintains a high degree of specificity towards glucose, its natural substrate. Sequence-specific hybridization of the tag strands with the address strands assembles each protein to its respective binding site, tethering the enzyme sufficiently close to the CNT to allow electron transfer when the redox potential is applied to the electrode. DNA hybridization is not the only means of protein attachment to the CNT array, however; we must also consider hydrophobic adsorption as an additional means of binding. It is well documented that proteins and DNA will bind non-covalently to hydrophobic surfaces such as CNT side-walls, primarily through hydrophobic interaction [2,4,5,26]. This

Fig. 2. (a) Quantity of GOx adsorbed to CNT side-walls vs. the quantity bound to CNTs by DNA hybridization, both before and after surfactant treatment. (b) Scan rate dependence of peak anodic (I_{pa}) and cathodic (I_{pc}) currents. Measurements taken at 25, 50, 100, 200 and 500 mV s^{-1} in 100 mM glucose resulted in peak oxidation currents of 0.547±0.008, 0.661±0.007, 0.945±0.012, 1.45±0.019 and 2.33±0.029, respectively, and peak reduction currents of −0.602±0.01, −0.891±0.013, −1.42±0.016, −2.24±0.025 and −3.75±0.041, respectively (n=5). Oxidation and reduction peak current plots are fit linearly, with r=0.989 and 0.986, respectively. (c) Anodic current peaks of CV measurements from the GOx–DNA–CNT system with glucose concentrations of (a) 0 mM, (b) 5 mM, (c) 10 mM, (d) 20 mM, (e) 50 mM and (f) 100 mM. Inset, plot of peak current vs. glucose concentration. (d) Anodic current peaks of CV measurements from the ADH–DNA–CNT system with varying ethanol concentrations (a) 0 mM, (b) 30 mM, (c) 60 mM, (d) 90 mM, (e) 150 mM and (f) 300 mM and 100 mM NAD. Inset, the plot of peak current vs. ethanol concentration. (e) Linear peak current response (the change in current from a 0 mM glucose baseline at 0.22 V vs. Ag/AgCl) in the glucose concentration range relevant for blood glucose monitoring in humans (marked by arrows), measured by CV. (f) Linear peak current response in the ethanol concentration range relevant for BAC monitoring in humans (0.08% BAC is marked by an arrow). Peak current (the change in current from a 0 mM ethanol baseline at 0.18 V vs. Ag/AgCl) is measured by CV in 100 mM NAD. (g) Peak current response of the GOx–DNA–CNT system from CV measurements taken once daily in 100 mM glucose. After 30 days and significant activity loss due to protein denaturation (arrows), the enzyme is removed by dehybridization in a DIH_2O bath at 65 °C, and fresh enzyme is hybridized to the sensor surface, restoring activity.

adsorption will cause both GOx and ADH to randomly attach to each others' designated nanoelectrode region, and effectively lead to a high level of background noise and false readings. It is critical to the design of the multifunctional protein nanochip that this type of random attachment be prevented. Many chemical surfactants have been proven to block protein adsorption, such as triton X-100, polyethylene glycol (PEG) and arabic gum (GA) [2,27,28]. To assess the effect of surfactant treatment on minimizing random protein adsorption, we first allowed GOx carrying a non-complementary DNA tag to adsorb extensively to seqA-modified CNTs. Using cyclic voltammetry (CV), we determined the surface coverage of adsorbed GOx to be $7.4\pm0.6\times10^{-13}$ mol cm^{-2} ($n=5$) by integrating the anodic current peak to find the total charge associated with the FAD redox units [20,21]. We then introduced GOx tagged with seqA' (GOx–seqA'), allowed the protein to link by DNA hybridization and found a surface coverage increase of $3.7\pm0.5\times10^{-13}$ mol cm^{-2} ($n=5$), representing the amount of enzyme hybridized to the array. We then repeated the experiment, this time after treating a seqA-modified CNT array with GA to resist protein adsorption. After surfactant treatment, the quantities of adsorbed and hybridized protein were found to be $7.1\pm1.7\times10^{-14}$ mol cm^{-2} ($n=5$) and $7.1\pm0.65\times10^{-13}$ mol cm^{-2} ($n=5$), respectively. These quantities are presented in Fig. 2a. In short, the surfactant treatment boosts the quantity of hybridized protein approximately twenty times relative to the quantity of adsorbed protein. The ratio of hybridized enzyme to adsorbed enzyme, which will dictate the signal-to-noise ratio in our multifunctional biosensor, improves from 1:2 to 10:1. The near two-fold increase in hybridization efficiency following surfactant treatment is also an interesting observation that may be attributed to reduced steric hindrance in the absence of adsorbed GOx.

3.2. Electrochemical characterization of DNA-linked enzyme–CNT biosensors

To characterize the glucose sensitivity of our DNA-assembled biosensor, GOx–seqA' was hybridized to a seqA-modified CNT array electrode subsection treated with GA, and CV measurements were taken at various scan rates and concentrations of glucose. The oxidation and reduction peak currents show a linear scan rate dependence (Fig. 2b), which is characteristic of a surface-controlled process [29]. Anodic current peaks exhibit an increasing current response with increasing glucose concentrations (Fig. 2c). Inset in this figure is the peak current response as a function of glucose concentration, measured from a 0 mM glucose baseline. Saturation of the system occurs around 50 mM. As a control, GOx–seqB' was added to a seqA-modified CNT array electrode subsection and subjected to hybridization conditions. The characteristic GOx redox peak did not appear in subsequent CV measurements, and no significant current increase was observed in response to glucose injections (data not shown), indicating that GOx–seqB' did not link to the non-complementary seqA-modified electrode. This result suggests that the DNA assembly of the biosensor is sequence-specific. Based on the GOx surface coverage of $6.72\pm0.51\times10^{-13}$ mol cm^{-2} (determined electrochemically as previously described, $n=5$) and a peak anodic current density of $1.69\pm0.15\times10^{-6}$ A cm^{-2} ($n=5$), we have calculated a unimolecular electron transfer rate (k_{ET}) of 14 ± 1.6 s^{-1}, using a method reported previously [2,22]. This value exceeds that of many directly-linked GOx–CNT biosensing systems reported by nearly an order of magnitude [3–7,30], indicating that the DNA link does not obstruct efficient electron transfer. We have observed this elevated rate of electron transfer in previous studies using highly ordered CNT array electrodes, and have attributed the effect to both the enhanced electron tunneling rate at the high-curvature CNT tips, and to the preservation of natural, active enzyme conformation at this small, hydrophilic point-of-contact [2]. For the analogous ADH system, ADH–seqB' was hybridized to a seqB-modified CNT array electrode subsection treated with GA, and CV measurements were taken at various ethanol concentrations. Anodic current peaks taken from these CV curves (Fig. 2d) show a direct ethanol concentration–peak current relationship. Inset in this figure is the peak current response as a function of ethanol concentration, measured from a 0 mM ethanol baseline. Saturation of the system occurs around 300 mM ethanol. Based on the ADH surface coverage of $1.24\pm0.1\times10^{-12}$ mol cm^{-2} and a peak anodic current density of $1.07\pm0.12\times10^{-5}$ A cm^{-2}, we calculate a unimolecular electron transfer rate (k_{ET}) of 23 ± 3.2 s^{-1}.

3.3. Utility of the DNA link

Though selected as proof-of-concept protein models, both the glucose and ethanol biosensors have relevant applications, including blood glucose monitoring in diabetes patients and blood alcohol content (BAC) determination. The normal concentration range of glucose in the human bloodstream is ~4 mM to 7 mM (70 to 130 mg/dl) [31]. Fig. 2e shows the glucose concentration–peak current relationship for the glucose sensor in and around this range, with the normal range limits marked by arrows. This relationship is highly linear both within and significantly outside these limits, fitting the line $a=1.24\times10^{-8}b$. The linearity of response in this range ensures reliable calibration and reading of the biosensor. Furthermore, the average standard deviation of 0.32 mM (5.8 mg/dl) easily exceeds the international standard of +/−20 mg/dl for glucose detection accuracy [32]. Fig. 2f shows the ethanol concentration–peak current relationship around the relevant range for BAC measurements, with the common point of legal intoxication (0.08 BAC) marked by an arrow. Again, the relationship is linear, fitting the line $a=4.53\times10^{-7}b$ with a standard deviation of +/−0.01%. This exceeds the generally accepted standard of accuracy for breathalyzer devices.

Both the glucose and ethanol biosensors therefore exceed the criteria as functional sensors for their respective analytes. The protein–DNA–CNT transducers remain approximately 70% active after daily use for 1 month. Fig. 2g shows the life cycle of a DNA-assembled GOx–CNT biosensor to demonstrate the renewability that the DNA link provides. After substantial activity loss (~30%), a heated DIH_2O dehybridization bath is used to remove old GOx–seqA', and fresh GOx–seqA' is bound in its place, restoring the original level of activity. This renewing of the protein bio-nanoelectronic system can be performed repeatedly, as the DNA address oligo modification does not appear to degrade over any timescale yet tested. Alternatively, following GOx–seqA' removal, ADH–seqA' can be bound in its place to change the functionality of the biosensor from glucose-sensing to ethanol-sensing (data not shown).

3.4. DNA-programmed multiplexing of the biosensor

The ultimate goal of this study is to demonstrate the use of the DNA link to site-specifically address the binding of different enzymes to isolated regions of the nanoelectrode surface to demonstrate scalable protein bio-nanoelectronic technology capable of monitoring the activity of multiple proteins and detecting the levels of multiple substances in real-time. To this end, we divided a CNT array chip into two subsections and gave each region a unique DNA address by treating one with seqA and the other with seqB, each having separate electric contacts at the backside of the CNT array. We then put the duplex chip in a hybridization bath containing a mixture of GOx–seqA' and ADH–seqB' and allowed each enzyme to find its place on the sensor surface relying on sequence-specific hybridization of the DNA link (Fig. 3a–b). Chronoamperometric measurements were then taken from each sensor region as glucose and ethanol were each injected at intervals. The glucose concentration is incremented by 5 mM at $t=10$ and 20 s, and the ethanol concentration is incremented by 20 mM at $t=5$ and 15 s, marked by red and blue arrows, respectively. Fig. 3c shows the current response of both the glucose

(red) and ethanol (blue) sensing regions. The GOx-linked region responds with a current step only to injections of glucose, while the region addressed for ADH attachment responds only to ethanol injections. The magnitude of the current steps in each case correlate closely to the peak currents observed during CV measurements at comparable substrate concentrations. As a control, a seqA-modified CNT electrode (no enzyme added) was found to have no current step response to either glucose or ethanol injections (Fig. 3c, gray).

4. Conclusions

In summary, the DNA molecular linking strategy we have devised has been shown to bind redox proteins to a CNT electrode surface in a sequence-specific manner, enabling addressable linking to discrete regions on the CNT array for multiplexed sensing. We have exploited the reversibility of DNA hybridization to remove inactive enzyme from the CNT array and replace it with fresh enzyme to renew and extend the lifetime of the system. Although reusability may not seem immediately beneficial to certain applications such as medical sensors which rely mostly on disposable technology, it is a feature that could prove tremendously useful for a great number of current and future applications in sectors such as academics, industry and defense, to name a few. These redox enzyme–CNT bio-nanoelectronic transducers have exhibited high k_{ET}s, indicating an efficient transfer of electrons across the DNA link. We have measured levels of sensitivity, accuracy and linear current response that are suitable to important biosensing applications such as blood glucose monitoring and BAC determination. Though two enzymes are chosen as demonstration vehicles in this work, the potential for scalability to many more proteins is evident. This scalable molecular linking scheme is suitable for any redox enzyme-based bioelectronics device, and can vastly facilitate the controllable and site-addressable assembly, disassembly and replacement of fragile bio-components by virtue of sequence-specific DNA hybridization.

Acknowledgement

This work was made possible by generous support from the AFOSR through the MURI program.

References

[1] D. Yao, H. Cao, S. Wen, D. Liu, Y. Bai, W. Zheng, A novel biosensor for sterigmatocystin constructed by multi-walled carbon nanotubes (MWNT) modified with aflatoxin-detoxifizyme (ADTZ), Bioelectrochemistry 68 (2006) 126–133.
[2] G.D. Withey, A.D. Lazareck, M.B. Tzolov, A. Yin, P. Aich, J.I. Yeh, J.M. Xu, Ultra-high redox enzyme signal transduction using highly ordered carbon nanotube array electrodes, Biosensors and Bioelectronics 21 (2006) 1560–1565.
[3] C. Cai, J. Chen, Direct electron transfer of glucose oxidase promoted by carbon nanotubes, Analytical Biochemistry 332 (2004) 75–83.
[4] A. Guiseppi-Elie, C. Lei, R.H. Baughman, Direct electron transfer of glucose oxidase on carbon nanotubes, Nanotechnology 13 (2002) 559–564.
[5] Y. Zhao, W. Zhang, H. Chen, Q. Luo, Direct electron transfer of glucose oxidase molecules adsorbed onto carbon nanotube powder microelectrode, Analytical Science 18 (2002) 939–941.
[6] X. Yu, D. Chattopadhyay, I. Galeska, F. Papadimitrakopoulos, J.F. Rusling, Peroxidase activity of enzymes bound to the ends of single-wall carbon nanotube forest electrodes, Electrochemistry Communications 5 (2003) 408–411.
[7] S. Sotiropoulou, N.A. Chainotakis, Carbon nanotube array-based biosensor, Analytical and Bioanalytical Chemistry 375 (2003) 103–105.
[8] E. Katz, A.F. Buckmann, I. Willner, Self-powered enzyme-based biosensors, Journal of the American Chemical Society 123 (2001) 10752–10753.
[9] S.C. Tsang, Y.K. Chen, P.J.F. Harris, M.L.H. Green, A simple chemical method of opening and filling carbon nanotubes, Nature 372 (1994) 159–162.
[10] B.R. Taft, A.D. Lazareck, G.D. Withey, A. Yin, J.M. Xu, S.O. Kelley, Site-specific assembly of DNA and appended cargo on arrayed carbon nanotubes, Journal of the American Chemical Society 126 (2004) 12750–12751.
[11] C. Boozer, J. Ladd, S. Chen, Q. Yu, J. Homola, S. Jiang, DNA directed protein immobilization on mixed ssDNA/oligo(ethylene glycol) self-assembled monolayers for sensitive biosensors, Analytical Chemistry 76 (2004) 6967–6972.
[12] S. Li, P. He, J. Dong, Z. Guo, L. Dai, DNA-directed self-assembling of carbon nanotubes, Journal of the American Chemical Society 127 (2005) 14–15.
[13] J. Li, C. Papadopoulos, J.M. Xu, Highly-ordered carbon nanotube arrays for electronics applications, Applied Physics Letters 75 (1999) 367–369.
[14] C. Godet, M. Boujtita, N.E. Murr, Direct electron transfer involving a large protein: glucose oxidase, New Journal of Chemistry 23 (1999) 795–797.
[15] S.G. Wang, Q. Zhang, R. Wang, S.F. Yoon, A novel multi-walled carbon nanotube-based biosensor for glucose detection, Biochemical and Biophysical Research Communications 311 (2003) 572–576.
[16] S.G. Wang, Q. Zhang, R. Wang, S.F. Yoon, J. Ahn, D.J. Yang, J.Z. Tian, J.Q. Li, Q. Zhou, Multi-walled carbon nanotubes for the immobilization of enzyme in glucose biosensors, Electrochemisty Communications 5 (2003) 800–803.
[17] J. Wang, M. Musameh, A reagentless amperometric alcohol biosensor based on carbon-nanotube/teflon composite electrodes, Analytical Letters 36 (2003) 2041–2048.
[18] J. Wang, Carbon-nanotube based electrochemical biosensors: a review, Electroanalysis 17 (2005) 7–14.
[19] C.M. Niemeyer, T. Sano, C.L. Smith, C.R. Cantor, Oligonucleotide-directed self-assembly of proteins: semisynthetic DNA-streptavidin hybrid molecules as connectors for the generation of macroscopic arrays and the construction of supramolecular bioconjugates, Nucleic Acids Research 22 (1994) 5530–5539.
[20] F. D ', L.M. Rogers, E.S. O, ' Dell, A. Kochman, W. Kutner, Immobilization and electrochemical redox behavior of cytochrome *c* on fullerene film-modified electrodes, Bioelectrochemistry 66 (2005) 35–40.
[21] . I. Willner, E. Katz, F. Patolsky, A.F. Buckmann, Biofuel cell based on glucose oxidase and microperoxidase-11 monolayer-functionalized electrodes, Journal of the Chemical Society, Perkin Transactions 2 8 (1998) 1817–1822.
[22] Y. Xiao, F. Patolsky, E. Katz, J.F. Hainfeld, I. Willner, Plugging into enzymes: nanowiring of redox enzymes by a gold nanoparticle, Science 299 (2003) 1877–1881.
[23] M. Bodanszky, A. Bodanszky, The Practice of Peptide Synthesis, 2nd edn.Springer, New York, 1994.
[24] L.A. Chrisey, G.U. Lee, C.E. O'Ferrall, Covalent attachment of synthetic DNA to self-assembled monolayer films, Nucleic Acids Research 24 (1996) 3031–3039.
[25] R.H. Garrett, C.M. Grisham, 2nd edn., Biochemistry, Harcourt, New York, 1999.
[26] M. Guo, J. Chen, D. Liu, L. Nie, S. Yao, Electrochemical characteristics of the immobilization of calf thymus DNA molecules on multi-walled carbon nanotubes, Bioelectrochemistry 62 (2004) 29–35.
[27] R. Bandyopadhyaya, E. Nativ-Roth, O. Regev, R. Yerushalmi-Rozen, Stabilization of individual carbon nanotubes in aqueous solutions, Nano Letters 2 (2002) 25–28.
[28] M. Shim, N.W.S. Kam, R.J. Chen, Y. Li, H. Dai, Functionalization of carbon nanotubes for biocompatibility and biomolecular recognition, Nano Letters 2 (2002) 285–288.
[29] Q. Lu, X. Chen, Y. Wu, S. Hu, Studies on direct electron transfer and biocatalytic properties of heme proteins in lecithin film, Biophysical Chemistry 117 (2005) 55–63.
[30] J.J. Gooding, R. Wibowo, J.Q. Liu, W. Yang, D. Losic, S. Orbons, F.J. Mearns, J.G. Shapter, D.B. Hibbert, Protein electrochemistry using aligned carbon nanotube arrays, Journal of the American Chemical Society 125 (2003) 9006–9007.
[31] J.E. Gerich, The importance of tight glycemic control, American Journal of Medicine 118 (2005) 7S–11S.
[32] International Organization for Standardization, Requirements for in vitro blood glucose monitoring systems for self-testing in managing diabetes mellitus, 2002 ISO/DIS 15197.